

A quantum embedding theory in the screened Coulomb interaction: Combining configuration interaction with GW /BSE

Marc Dvorak,* Dorothea Golze, and Patrick Rinke

Department of Applied Physics, Aalto University School of Science, 00076-Aalto, Finland

(Dated: October 30, 2018)

We present a new quantum embedding theory called dynamical configuration interaction (DCI) that combines wave function and Green's function theories. DCI captures static correlation in a correlated subspace with configuration interaction and couples to high-energy, dynamic correlation outside the subspace with many-body perturbation theory based on Green's functions. In the correlated subspace, we use a wave function description to avoid embedding the two-particle vertex, which greatly simplifies the frequency structure of the embedding. DCI takes the strengths of both theories to balance static and dynamic correlation in a single, fully *ab-initio* embedding concept. We show that treating high-energy correlation up to the GW and Bethe-Salpeter equation level is sufficient even for challenging multi-reference problems. Our theory treats ground and excited states on equal footing, and we compute the dissociation curve of N_2 , vertical excitation energies of N_2 and C_2 , and the ionization spectrum of benzene in excellent agreement with high level quantum chemistry methods and experiment.

The prediction of both ground and excited states of quantum many-body systems remains one of the most challenging and intensely researched topics in physics, materials science, and chemistry. While independent electron theories give successful predictions for weakly-correlated molecules and materials, there is increasing interest in strongly-correlated systems, perhaps with *d*- or *f*-electrons,¹ that are poorly described by mean-field theories. Such molecules and materials host interesting physics driven by electronic correlation, including magnetism or Kondo physics, and have great potential for new applications.

The importance of the quantum many-body problem is accentuated by its highly multi-disciplinary nature. Diversity arises from the dramatic variation of electronic correlation: from the highly multi-reference character along reaction pathways in quantum chemistry to dynamical screening in single-reference, polarizable materials. Theories from different disciplines describe certain regimes of correlation better than others, with widely varying computational costs.² Accordingly, there is great potential for new methods which combine theories to enhance their respective strengths and downplay their weaknesses. Methods which merge disciplines could achieve a balance between accuracy and computational cost not attainable within any one field.

Quantum embedding³ is one approach to the strongly-correlated problem. The general idea of a strongly-correlated impurity, or embedded region, coupled to a weakly-interacting bath is a notorious and difficult problem in physics.⁴ The distinction between the impurity and bath make embedding theories a natural candidate for combining two different methods. However, fully *ab-initio* embedding theories that are still computationally feasible are difficult to derive. Exact embedding frameworks exist^{5,6} but, without any simplification, are essentially as intractable as the initial many-body problem. Approximate model Hamiltonians⁷⁻⁹ are useful to reduce the computational cost but may rely on semi-empirical

or otherwise not *ab-initio* parameters. Developing rigorous, fully *ab-initio* – and yet approximate – theories is a challenge.¹⁰

Exact diagonalization (ED) of the many-body Hamiltonian is the standard by which all other methods are measured.¹¹ ED, or its truncated basis version configuration interaction (CI), is extremely expensive. However, ED naturally describes all ranges of static correlation or multi-reference character in a frequency independent framework. At the other end of the correlation spectrum, many-body perturbation theory^{12,13} (MBPT) based on Green's functions efficiently describes dynamic correlation, or correlation among high-energy degrees of freedom. In particular, the GW approximation¹⁴ and Bethe-Salpeter equation¹⁵ (BSE) are very successful at predicting quasiparticle excitations in weakly- to moderately-correlated materials.¹⁶⁻²² However, static correlation in the Green's function formalism requires the treatment of difficult frequency dependent kernels.

In this Letter, we highlight a new quantum embedding theory to merge these complementary disciplines. First, we partition the Hilbert space into strongly- and weakly-correlated portions, equivalent to low- and high-energy transitions, defined by an orbital active space (AS). The many-body Hamiltonian in the low-energy subspace is diagonalized with configuration interaction. Additionally, we downfold the effects of high-energy transitions onto a dynamical correction added to the CI Hamiltonian. We estimate these dynamical corrections with a modified GW /BSE procedure. Our energy dependent corrections correlate the full set of orbitals *beyond* the orbital AS and efficiently include dynamic correlation from the bath. Our dynamical configuration interaction (DCI) theory takes advantage of the strengths of these two theories: we treat dynamic correlation with GW /BSE and static correlation with CI.

Details of the theory are contained in a separate publication.²³ Here, we outline the theory and present the major results. We consider the exact,

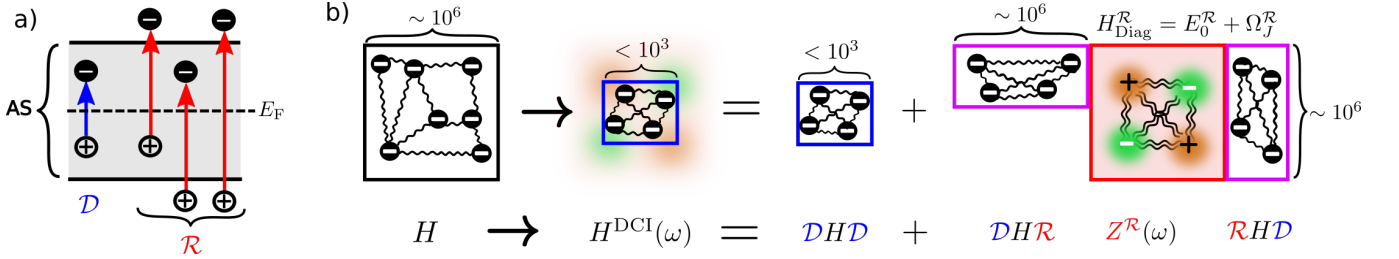


FIG. 1. a) Partitioning of the many-body Hilbert space into \mathcal{D} (blue) and \mathcal{R} (red). All excitations that fall inside the orbital AS, shaded in grey, belong to \mathcal{D} . All other configurations are placed in \mathcal{R} . b) The downfolding procedure reduces the size of the matrix diagonalization from $\sim 10^6$ to $< 10^3$ for the systems studied here. Matrix elements of the exact H describe N interacting bare electrons (black) in the vacuum (white background). The renormalized $H^{\mathcal{R}}$, which we limit to a diagonal approximation, describes $2m$ ($m = \text{excitation level}$) interacting quasiparticles (orange and green) above a correlated ground state (red background).

non-relativistic, electronic Hamiltonian in the Born-Oppenheimer approximation.

$$H = \sum_{ij}^N t_{ij} a_i^\dagger a_j + \sum_{ijkl}^N v_{ijkl} a_i^\dagger a_j^\dagger a_l a_k \quad (1)$$

t_{ij} and v_{ijkl} are the one- and two-body (Coulomb) matrix elements of the Hamiltonian and a_i (a_j^\dagger) are fermionic destruction (creation) operators.

We start the embedding construction by dividing the many-body Hilbert space into two portions, which we denote \mathcal{D} and \mathcal{R} . \mathcal{D} and \mathcal{R} are projection operators defined so that their sum equals the identity,

$$\mathcal{D} = \sum_I |I\rangle \langle I| \quad ; \quad \mathcal{R} = \sum_J |J\rangle \langle J| \quad ; \quad \mathbf{I} = \mathcal{D} + \mathcal{R}. \quad (2)$$

Here, $|I\rangle$ and $|J\rangle$ are many-body configurations. To connect the many-body projectors to the single-particle picture, we define an orbital AS around the Fermi energy, as shown in Fig. 1a. The AS contains the statically correlated single-particle states. We place all many-body configurations $|I\rangle$ containing AS excitations in the strongly-correlated space, \mathcal{D} . This criterion includes all excitation levels (single, double, etc.). We place all other configurations $|J\rangle$ in the weakly-correlated space, \mathcal{R} , which contains only high-energy degrees of freedom.

Based on the projectors, the Schrödinger equation can be downfolded onto an effective Hamiltonian in \mathcal{D} :

$$\begin{aligned} Z^{\mathcal{R}}(E) &= \frac{1}{E - \mathcal{R}H\mathcal{R}} \\ M(E) &\equiv [\mathcal{D}H\mathcal{R}] Z^{\mathcal{R}}(E) [\mathcal{R}H\mathcal{D}] \\ H^{\text{eff}}(E) \phi &= [\mathcal{D}H\mathcal{D} + M(E)] \phi = E\phi. \end{aligned} \quad (3)$$

This is the Löwdin or Feshbach-Schur decomposition, demonstrated in Fig. 1b, and is an exact rewriting of the Hamiltonian.^{6,24-31} The effect of the downfolding is to add an energy dependent correction, $M(E)$, to the subspace Hamiltonian $\mathcal{D}H\mathcal{D}$. The non-linear Hamiltonian in Eq. 3 must be iterated to find each eigenvalue E self-consistently.

Eq. 3 introduces the resolvent of the projected Hamiltonian $\mathcal{R}H\mathcal{R}$, here labeled $Z^{\mathcal{R}}(E)$, which is the crucial ingredient coupling the two spaces. By downfolding, the effective Hamiltonian has been dramatically reduced in size to $\dim\mathcal{D}$, but the nonlinear eigenvalue problem in Eq. 3 is still very expensive. Computing the resolvent depends on the inversion of the enormous $\mathcal{R}H\mathcal{R}$ block of the Hamiltonian. For a realistic problem, \mathcal{R} can be many orders of magnitude larger than \mathcal{D} .

Our theory transforms the projected $\mathcal{R}H\mathcal{R}$ Hamiltonian to make $Z^{\mathcal{R}}(E)$ easier to compute. Consider rewriting the full Hamiltonian in Eq. 1 as a ground state energy plus excitations,

$$H = E_0 + \Omega, \quad (4)$$

where E_0 is the correlated ground state energy and Ω is an excitation matrix with eigenvalues equal to excitation energies of the system. In wave function theories, excitation energies are computed as total energy differences so that $\Omega = H - E_0$. However, Green's function theories directly compute excitation energies by diagonalizing effective quasiparticle (QP) Hamiltonians, Ω^{QP} . As long as the QP excitations are long-lived, we can approximate exact excitation energies of Ω by Ω^{QP} .

In the same spirit, we renormalize the exact $\mathcal{R}H\mathcal{R}$ to a Hamiltonian of excitations propagating over a correlated ground state. By introducing a ground state energy in \mathcal{R} , which we denote $E_0^{\mathcal{R}}$, we separate eigenstates of $\mathcal{R}H\mathcal{R}$ into a ground state and excitation energy. We rewrite $\mathcal{R}H\mathcal{R}$ as

$$\mathcal{R}H\mathcal{R} \rightarrow H^{\mathcal{R}} \equiv E_0^{\mathcal{R}} + \Omega^{\mathcal{R}} \quad (5)$$

for some ground state energy $E_0^{\mathcal{R}}$ and excitation matrix $\Omega^{\mathcal{R}}$. $E_0^{\mathcal{R}}$ and $\Omega^{\mathcal{R}}$ are constructed to connect to the physical ground state E_0 and physical excitation matrix Ω by increasing the size of \mathcal{R} .

If we can separately compute $E_0^{\mathcal{R}}$ and $\Omega^{\mathcal{R}}$, and for less expense than inverting $\mathcal{R}H\mathcal{R}$, we can assemble them to write the Hamiltonian as in Eq. 5. We make a QP approximation to $\Omega^{\mathcal{R}}$ to set up a calculation with MBPT.

Even in a diagonal approximation, QP Hamiltonians correlate the full set of orbitals through intermediate sums in the diagrammatic expansion. For this reason, and to lower the expense of inverting $\mathcal{R}H\mathcal{R}$, we adopt a diagonal approximation to the Hamiltonian $H^{\mathcal{R}}$. After we also estimate the energy $E_0^{\mathcal{R}}$, we insert the renormalized $H^{\mathcal{R}}$ in place of $\mathcal{R}H\mathcal{R}$ in Eq. 3. The ensuing inversion of the diagonal matrix is trivial and still describes \mathcal{R} correlation at the quasiparticle level. Our approach is *not* an application of perturbation theory based on the residual potential $U \equiv v - v^{\text{MF}}$, as in Møller-Plesset perturbation theory, nor is it Green's function embedding with a high accuracy CI impurity solver.^{32,33}

Neutral excitation energies in MBPT are ordinarily computed with the BSE. However, the basis of single excitations for the BSE does not match the CI basis, which contains many-body configurations up to all excitation levels. In order to easily calculate multiple excitation energies and match the CI basis, we construct a correlation function which explicitly considers multiple excitations in \mathcal{R} , denoted $\mathcal{L}^{\mathcal{R}}$.³⁴

$$\mathcal{L}_{J,J'}^{\mathcal{R}}(t;t') = \langle \Psi^{\mathcal{R}} | T[\hat{\Omega}_J^{\mathcal{R}} \hat{\Omega}_{J'}^{\mathcal{R}\dagger}] | \Psi^{\mathcal{R}} \rangle + \mathcal{G}_0^{\mathcal{R}}. \quad (6)$$

The operator $\hat{\Omega}_{J'}^{\mathcal{R}\dagger}$ ($\hat{\Omega}_J^{\mathcal{R}}$) creates (destroys) the \mathcal{R} configuration $|J'\rangle$ ($|J\rangle$) at time t' (t). $\hat{\Omega}_{J'}^{\mathcal{R}\dagger}$ can take any excitation level. $\Psi^{\mathcal{R}}$ is a fictitious ground state in the \mathcal{R} subspace with energy $E_0^{\mathcal{R}}$, discussed in detail in our complementary publication.²³ Because the outer lines of $\mathcal{L}^{\mathcal{R}}$ take all excitation levels, we can estimate all multiple excitation energies in a frequency independent framework. We systematically apply MBPT with the *projected* Hamiltonian $\mathcal{R}H\mathcal{R}$ in the *full* many-body basis for successively improved approximations to $\mathcal{L}^{\mathcal{R}}$.

An \mathcal{R} excitation $\hat{\Omega}_{J'}^{\mathcal{R}\dagger}$ of level m contains m propagating electrons and m propagating holes. To estimate the energies of the $2m$ independent quasiparticles, we dress each particle with a self-energy based on the GW approximation.^{14,35–37} We adopt the constrained random phase approximation (cRPA) for the polarization to constrain the correlation to the \mathcal{R} subspace. In the cRPA, only \mathcal{R} transitions screen the Coulomb interaction, denoted $W_{\mathcal{R}}$. The cRPA is already established as an effective tool in strongly-correlated physics and quantum embedding for determining effective low-energy parameters.^{38–42} In this approximation, the quasiparticle self-energy is $\Sigma = iGW_{\mathcal{R}}$. In the limits $\mathcal{D} \rightarrow \mathbf{I}$ or $\mathcal{R} \rightarrow \mathbf{I}$, self-energies in the $GW_{\mathcal{R}}$ approximation correctly approach the Hartree-Fock (HF) or full GW limits of CI or MBPT, respectively. We also include inter-quasiparticle (e-h, e-e, h-h) interactions based on the same partially screened interaction, $W_{\mathcal{R}}$, similar to the electron-hole interaction of the BSE.^{43,44}

To avoid introducing a second frequency dependence to the Hamiltonian, we must remove the frequency dependence of $\mathcal{L}^{\mathcal{R}}$. For this reason, we adopt the same set of static approximations commonly applied to the BSE, in which outer lines are evaluated at their quasiparticle

energies and their interaction via $W_{\mathcal{R}}$ is taken at zero frequency. The perturbation expansion for $\mathcal{L}^{\mathcal{R}}$ gives an effective $2m$ -particle Hamiltonian – the excitation matrix $\Omega^{\mathcal{R}}$ – taken from the denominator of $\mathcal{L}^{\mathcal{R}}$. We estimate \mathcal{R} excitation energies with diagonal elements of this Hamiltonian in the static approximation. The excitation energy, denoted $\Omega_J^{\mathcal{R}}$ (without the operator hat), for the excitation created by $\hat{\Omega}_J^{\mathcal{R}\dagger}$ is

$$\begin{aligned} \Omega_J^{\mathcal{R}} &= \langle J | \Omega^{\mathcal{R}} | J \rangle \\ &= \sum_{e \in J} \epsilon_e^{GW_{\mathcal{R}}} - \sum_{h \in J} \epsilon_h^{GW_{\mathcal{R}}} \\ &\quad + \sum_{e,h \in J} (-W_{\mathcal{R},ehhe} + \delta_{\sigma_e \sigma_h} v_{ehhe}) \\ &\quad + \sum_{\substack{e \in J \\ e \neq e'}}^m (W_{\mathcal{R},ee'e'e} - \delta_{\sigma_e \sigma_{e'}} W_{\mathcal{R},ee'e'e}) \\ &\quad + \sum_{\substack{h \in J \\ h \neq h'}}^m (W_{\mathcal{R},hh'h'h} - \delta_{\sigma_h \sigma_{h'}} W_{\mathcal{R},hh'h'h}). \end{aligned} \quad (7)$$

In Eq. 7, e and h denote electrons and holes in configuration $|J\rangle$, σ is a spin variable, and sums run up to the excitation level m of the configuration. A crude schematic of these inter-quasiparticle interactions is shown in Fig. 1b.

We must also compute the ground state energy $E_0^{\mathcal{R}}$ to complete the transformation. This poses a theoretical challenge since both the reference configuration and real ground state are, in practice, always placed in \mathcal{D} . We follow a simple guiding principle for $E_0^{\mathcal{R}}$, as with $\Omega^{\mathcal{R}}$, which is to enforce the correct limits as $\mathcal{R} \rightarrow \mathbf{I}$ or $\mathcal{D} \rightarrow \mathbf{I}$. Our procedure to estimate $E_0^{\mathcal{R}}$ is described elsewhere,²³ but we emphasize here that it is fully *ab-initio* and free of any adjustable parameters.

With the excitation matrix and ground state energy in hand, we can write the $H^{\mathcal{R}}$ Hamiltonian of Eq. 5. After inserting $H^{\mathcal{R}}$ in place of $\mathcal{R}H\mathcal{R}$ in the resolvent, the final effective equations are

$$\begin{aligned} M_{II'}(\omega) &= \sum_J \langle I | H | J \rangle \frac{1}{(\omega - \Delta) - \Omega_J^{\mathcal{R}}} \langle J | H | I' \rangle \\ H_{II'}^{\text{DCI}}(\omega) &= \langle I | H | I' \rangle + M_{II'}(\omega) \end{aligned} \quad (8)$$

where $\omega \equiv E - E_0$ and Δ , which is on the scale of a correlation energy, is related to the calculation of $E_0^{\mathcal{R}}$. Our dynamical configuration interaction (DCI) Hamiltonian in Eq. 8 represents a subspace wave function dynamically embedded in a bath of interacting quasiparticles. The matrix elements $\langle I | H | I' \rangle$ and $\langle I | H | J \rangle$ are computed with the exact many-body Hamiltonian using the Slater-Condon rules.^{45,46} Compared to Eq. 3, we have renormalized quantities in the denominator of $Z^{\mathcal{R}}(\omega)$ to excitation energies, though the eigenvalue of H^{DCI} is still the total energy. For the ground state, ω is set to zero and no self-consistent iterations are needed. For excited states, the excitation energy must be found self-consistently by

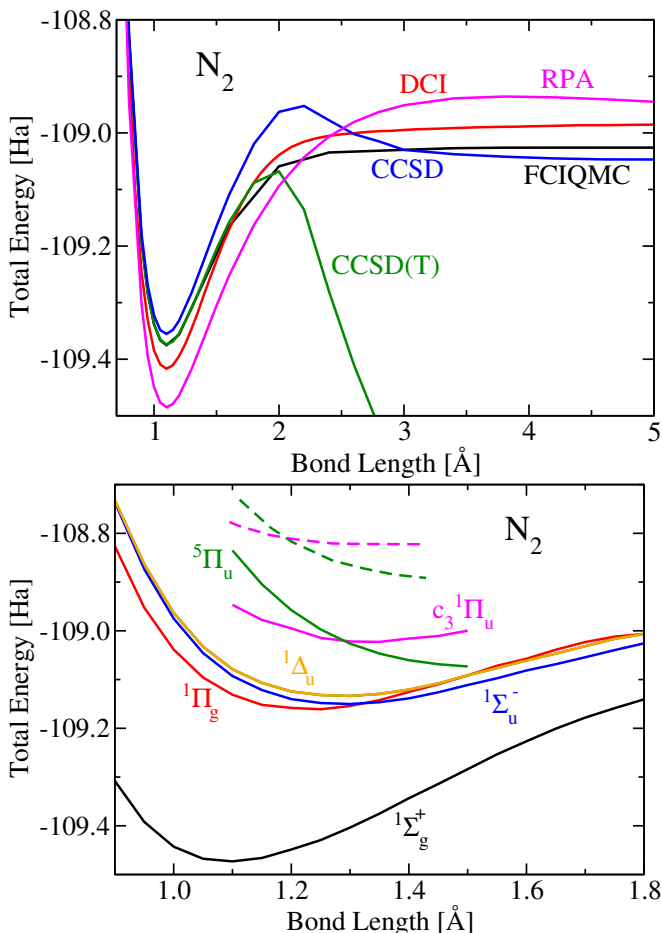


FIG. 2. Top: Dissociation curve of the N_2 dimer computed with DCI (6, 6) in the cc-pVTZ⁵⁵ basis set compared against exact results (FCIQMC), RPA, CC with single and double excitations (CCSD), and CCSD with perturbative triple excitations (CCSD(T)). Reference data taken from Ref. 56. Bottom: DCI excited state energy surfaces computed with the cc-pVQZ basis. Our DCI calculations do not use symmetry and we take the state labeling from Ref. 48. Dashed lines are FCI results from Ref. 48 in the cc-pVDZ basis set. The vertical offset is primarily due to the different basis sets, and only the curve shapes and intersection are meant for comparison.

iterating Eq. 8 until the excitation energy, $\Omega_i = E_i - E_0$, equals the evaluation energy, $\omega = \Omega_i$.

We first test the theory by dissociating the N_2 dimer in the triple-bond AS. Bond breaking of molecular dimers is a challenging multi-reference problem because the correct ground state wave function cannot be written as a single Slater determinant.^{28,47–49} We perform DCI calculations by exactly diagonalizing the (6, 6) AS (6 electrons distributed in 6 spatial orbitals) dynamically embedded in the full set of molecular orbitals. Our calculations based on FHI-AIMS^{50–54} always use a HF starting point with $G_0W_0, \mathcal{R}@HF$ in the basis of HF orbitals.

Fig. 2 shows our DCI results compared to two versions of coupled cluster (CC), random phase approximation (RPA), and full configuration interaction quantum

Monte Carlo (FCIQMC). Our first observation is that DCI is free of unphysical bumps or divergences in the dissociation curve characteristic of single-reference methods such as CC. At equilibrium, DCI overestimates dynamic correlation compared to FCIQMC but is still an improvement over RPA at modest computational increase. DCI overestimates the total energy in the dissociation limit, but the dissociation curve is flat. The result, particularly in the multi-reference regime at dissociation, should improve by increasing the AS from the minimal (6, 6) space. The overall agreement with high level results is satisfactory considering the relative ease of our augmented (6, 6) CI calculation, which requires no multi-configurational orbital optimization, has a simple frequency dependence, and has no density functional dependence.

Next we consider excited states, which we expect to be the major strength of the theory. Total energies computed with DCI may inherit errors of the underlying MBPT calculation, which will always be subject to some approximation. However, our internally consistent treatment of correlation and balanced generation of determinants could perform better for excitation energies than total energies. Systematic errors in total energies for both ground and excited states may cancel during internal ω iterations to compute Ω . The accuracy of individual excitation energies or excited state spectra, instead of total energies, is most relevant for many applications.

Continuing with the challenging case of N_2 , we compute excited state energy surfaces along the dissociation path, shown in Fig. 2. Qualitatively, the ground state and three lowest excited states closely match FCI results.⁴⁸ Our primary interest is with the conical intersection between the higher energy $5\Pi_u$ and $c_3 1\Pi_u$ states near 1.3 Å. FCI results of this intersection from Ref. 48 are shown in Fig. 2 with dashed lines. There is a vertical shift between DCI and FCI data, which is mostly attributed to their different basis sets, but the shape of the DCI intersection agrees with the FCI results. All variants of CC considered in Ref. 48 miss this intersection. Properly describing the conical intersection demonstrates that DCI is unbiased towards any single \mathcal{D} configuration and can treat near degeneracies among multi-configurational states.

For a quantitative comparison, we report equilibrium excitation energies in Table I. Our DCI calculations show good agreement with experiment and equation-of-motion CC (EOM-CCSD). Different versions of GW/BSE all underestimate the excitation energy of N_2 ,⁵⁷ with the best estimate shown in Table I. The carbon dimer is a similarly challenging balance of multi-reference character combined with dynamic correlation. The lowest excitation energy for C_2 calculated with DCI, shown in Table I, is also in excellent agreement with benchmark data.

Finally, we consider a single-reference, dynamically correlated system. The ionization spectrum of benzene is a difficult prediction for GW and beyond- GW methods in MBPT. Self-consistency, vertex corrections, and mean-field starting points all have an effect on the re-

TABLE I. Vertical singlet excitation energies (eV) of N_2 ⁵⁷ and C_2 ^a computed with the Bethe-Salpeter equation (GW/BSE), EOM-CCSD,^{57,58} and DCI. Our (6,6) DCI calculations are performed at the experimental bond lengths of 1.0977 Å and 1.2425 Å, respectively, in the cc-pVQZ basis. EOM-CCSD calculations from Refs. 57 and 58 are numerically close to each other for N_2 .

| | GW/BSE | EOM-CCSD | DCI | Exp. ⁵⁹ |
|------------------|----------|----------|--------------|--------------------|
| $N_2 - \Omega_1$ | 7.93 | 9.47 | 9.33 | 9.31 |
| $N_2 - \Omega_2$ | 8.29 | 10.08 | 10.45 | 9.97 |
| $C_2 - \Omega_1$ | < 0.1 | 1.33 | 1.28 | 1.23 |

^a We perform our own calculation for C_2 at the $G_0W_0@HF/BSE$ level. The N_2 value from Ref. 57 is based on $G_0W_0@LDA/BSE$.

sulting spectrum.^{60,61} To describe the first 5 ionization energies, we use an orbital AS of (10, 7) and (9, 7) for the neutral molecule and ion, respectively. With these active spaces, correlation among the 5 highest occupied states and doubly degenerate LUMO is included nonperturbatively. However, the full π - σ space is much larger than these 7 orbitals. The correlation treatment in \mathcal{R} is therefore very important, and using such a small AS for benzene is a demanding test of the theory.

Our DCI prediction is shown in Fig. 3. The first ionization potential (IP), a bonding π state near 9 eV, is in good agreement with experiment and past results. DCI splits this π state into two peaks, in agreement with experiment and an improvement over EOM-CCSD results. The IP, computed as the difference between ground state energies of the ion and neutral molecule, is a different type of excitation than those considered so far. The IP depends on two different SCF and $GW_{\mathcal{R}}$ calculations (neutral and ion), so that the total energy difference does not depend on internal iterations of ω . It is encouraging that the theory can describe such a charged excitation. The π state near 12.5 eV is also in good agreement with experiment. We predict the first σ state to be ~ 0.15 eV below the closest π state. While this peak position is not perfectly aligned with experiment, it is in good agreement with recent EOM-CCSD results⁶² (< 0.2 eV). Studying this difficult σ state,^{60,61} which is impervious to G_0W_0 , $scGW$, EOM-CCSD, and DCI, is a topic worthy of further investigation. Our overall agreement with both experiment and EOM-CCSD is excellent considering our theory has no adjustable parameters which can be tuned to match the experimental result.

In conclusion, we have presented a new quantum embedding theory that effectively embeds a wave function calculation inside of a many-body Green’s function calculation. Our DCI theory merges aspects of quantum chemistry, strongly-correlated physics, and GW theory to provide a balanced, multi-disciplinary description of electronic correlation. By using a wave function description in \mathcal{D} , we avoid embedding the two-particle vertex which is intrinsic to Green’s function embedding. In \mathcal{R} , we apply MBPT in the unfolded basis for an efficient cal-

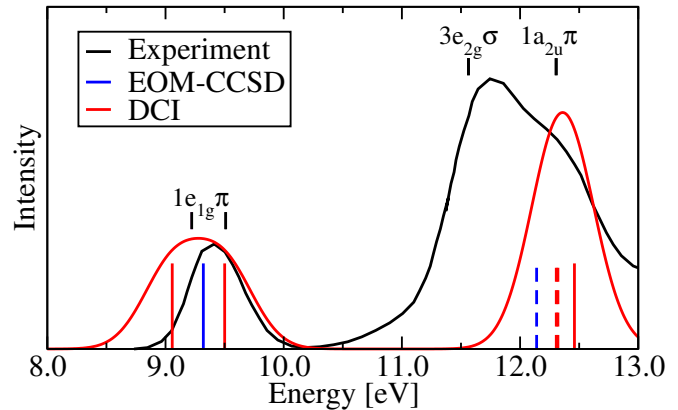


FIG. 3. Ionization spectrum of benzene measured by experiment⁶³ (black), and computed with DCI (red) and EOM-CCSD⁶² (blue). Peak assignments are taken from Ref. 64. We use the cc-pVDZ basis and generate \mathcal{D} up to triple excitations, CISDT. π states are indicated with solid lines while σ states are shown with dashed lines. There is no reported EOM-CCSD value for the highest π state.

ulation of multiple excitations with a static kernel. Initial calculations for dimers and benzene demonstrate the versatility of the theory for describing different regimes of correlation.

This work is supported by the Academy of Finland through grant Nos. 284621, 305632, 316347 and 316168. The authors acknowledge the CSC-IT Center for Science, Finland, for generous computational resources and the Aalto University School of Science “Science-IT” project for computational resources. The authors acknowledge A. Harju for early discussions on the topic, as well as fruitful discussions with S. Biermann, R. van Leeuwen, and Y. Pavlyukh.

* marc.dvorak@aalto.fi

¹ S. Choi, A. Kutepov, K. Haule, M. van Schilfhaarde, and G. Kotliar, NPJ Quant. Mat. **1** (2016).

² M. Motta, D. M. Ceperley, G. K.-L. Chan, J. A. Gomez, E. Gull, S. Guo, C. A. Jiménez-Hoyos, T. N. Lan, J. Li, F. Ma, A. J. Millis, N. V. Prokof’ev, U. Ray, G. E. Scuseria, S. Sorella, E. M. Stoudenmire, Q. Sun, I. S. Tupitsyn,

S. R. White, D. Zgid, and S. Zhang (Simons Collaboration on the Many-Electron Problem), Phys. Rev. X **7**, 031059 (2017).

³ Q. Sun and G. K.-L. Chan, Acc. Chem. Res. **49**, 2705 (2016).

⁴ P. W. Anderson, Phys. Rev. **124**, 41 (1961).

⁵ F. Aryasetiawan, J. M. Tomczak, T. Miyake, and

- R. Sakuma, Phys. Rev. Lett. **102**, 176402 (2009).
- ⁶ P. Löwdin, J. Math. Phys. **3**, 969 (1962).
 - ⁷ J. Hubbard, Proc. Roy. Soc. London A: Math., Phys. and Eng. Sci. **276**, 238 (1963).
 - ⁸ M. Bockstedte, F. Schütz, T. Garratt, V. Ivády, and A. Gali, NPJ Quant. Mat. **3**, 31 (2018).
 - ⁹ V. Ivády, R. Armiento, K. Szász, E. Janzén, A. Gali, and I. A. Abrikosov, Phys. Rev. B **90**, 035146 (2014).
 - ¹⁰ M. Casula, P. Werner, L. Vaugier, F. Aryasetiawan, T. Miyake, A. J. Millis, and S. Biermann, Phys. Rev. Lett. **109**, 126408 (2012).
 - ¹¹ T. Helgaker, P. Jørgensen, and J. Olsen, *Molecular electronic structure theory*, 1st ed. (John Wiley & Sons, Ltd, 2014).
 - ¹² R. M. Martin, L. Reining, and D. M. Ceperley, *Interacting Electrons: Theory and Computational Approaches* (Cambridge University Press, 2016).
 - ¹³ A. L. Fetter and J. D. Walecka, *Quantum Theory of Many-Particle Systems* (McGraw-Hill, Boston, 1971).
 - ¹⁴ L. Hedin, Phys. Rev. **139**, A796 (1965).
 - ¹⁵ E. E. Salpeter and H. A. Bethe, Phys. Rev. **84**, 1232 (1951).
 - ¹⁶ M. S. Hybertsen and S. G. Louie, Phys. Rev. B **34**, 5390 (1986).
 - ¹⁷ M. Rohlfing and S. G. Louie, Phys. Rev. B **62**, 4927 (2000).
 - ¹⁸ M. J. van Setten, F. Caruso, S. Sharifzadeh, X. Ren, M. Scheffler, F. Liu, J. Lischner, L. Lin, J. R. Deslippe, S. G. Louie, C. Yang, F. Weigend, J. B. Neaton, F. Evers, and P. Rinke, J. Chem. Theory Comput. **11**, 5665 (2015).
 - ¹⁹ D. Jacquemin, I. Duchemin, and X. Blase, J. Chem. Theory Comput. **11**, 3290 (2015).
 - ²⁰ F. Bruneval, S. M. Hamed, and J. B. Neaton, J. Chem. Phys. **142**, 244101 (2015).
 - ²¹ M. L. Tiago and J. R. Chelikowsky, Phys. Rev. B **73**, 205334 (2006).
 - ²² S. Körbel, P. Boulanger, I. Duchemin, X. Blase, M. A. L. Marques, and S. Botti, J. Chem. Theory Comput. **10**, 3934 (2014).
 - ²³ M. Dvorak and P. Rinke, arXiv (2018).
 - ²⁴ P. Löwdin, Int. J. Quan. Chem. **2**, 867 (1968).
 - ²⁵ V. A. Dzuba, V. V. Flambaum, and M. G. Kozlov, Phys. Rev. A **54**, 3948 (1996).
 - ²⁶ Y. Pavlyukh, M. Schüler, and J. Berakdar, Phys. Rev. B **91**, 155116 (2015).
 - ²⁷ V. A. Dzuba, J. C. Berengut, C. Harabati, and V. V. Flambaum, Phys. Rev. A **95**, 012503 (2017).
 - ²⁸ G. L. Manni, F. Aquilante, and L. Gagliardi, J. Chem. Phys. **134**, 034114 (2011).
 - ²⁹ G. Li Manni, D. Ma, F. Aquilante, J. Olsen, and L. Gagliardi, J. Chem. Theory Comput. **9**, 3375 (2013).
 - ³⁰ D. Sangalli, P. Romaniello, G. Onida, and A. Marini, J. Chem. Phys. **134**, 034115 (2011).
 - ³¹ P. Romaniello, D. Sangalli, J. A. Berger, F. Sottile, L. G. Molinari, L. Reining, and G. Onida, J. Chem. Phys. **130**, 044108 (2009).
 - ³² Y. Pavlyukh and W. Hübner, Phys. Rev. B **75**, 205129 (2007).
 - ³³ D. Zgid, E. Gull, and G. K.-L. Chan, Phys. Rev. B **86**, 165128 (2012).
 - ³⁴ The G_0^R term in Eq. 6 is meant to remove the non-propagating portion of the Green's function. We only keep the portion for the perturbation expansion which propagates in time.
 - ³⁵ G. Onida, L. Reining, and A. Rubio, Rev. Mod. Phys. **74**, 601 (2002).
 - ³⁶ F. Aryasetiawan and O. Gunnarsson, Rep. Prog. Phys. **61**, 237 (1998).
 - ³⁷ P. Rinke, A. Qteish, J. Neugebauer, C. Freysoldt, and M. Scheffler, New J. Phys. **7**, 126 (2005).
 - ³⁸ F. Aryasetiawan, M. Imada, A. Georges, G. Kotliar, S. Biermann, and A. I. Lichtenstein, Phys. Rev. B **70**, 195104 (2004).
 - ³⁹ E. Şaşıoğlu, C. Friedrich, and S. Blügel, Phys. Rev. B **83**, 121101 (2011).
 - ⁴⁰ L. Vaugier, H. Jiang, and S. Biermann, Phys. Rev. B **86**, 165105 (2012).
 - ⁴¹ M. Hirayama, T. Miyake, M. Imada, and S. Biermann, Phys. Rev. B **96**, 075102 (2017).
 - ⁴² H. Shinaoka, M. Troyer, and P. Werner, Phys. Rev. B **91**, 245156 (2015).
 - ⁴³ T. Deilmann, M. Drüppel, and M. Rohlfing, Phys. Rev. Lett. **116**, 196804 (2016).
 - ⁴⁴ T. Deilmann and K. S. Thygesen, Phys. Rev. B **96**, 201113 (2017).
 - ⁴⁵ J. C. Slater, Phys. Rev. **34**, 1293 (1929).
 - ⁴⁶ E. U. Condon, Phys. Rev. **36**, 1121 (1930).
 - ⁴⁷ A. Szabo and N. S. Ostlund, *Modern Quantum Chemistry: Introduction to Advanced Electronic Structure Theory*, 1st ed. (Dover Publications, Inc., Mineola, 1996).
 - ⁴⁸ H. Larsen, J. Olsen, P. Jørgensen, and O. Christiansen, J. Chem. Phys. **113**, 6677 (2000).
 - ⁴⁹ T. Olsen and K. S. Thygesen, J. Chem. Phys. **140**, 164116 (2014).
 - ⁵⁰ V. Blum, R. Gehrke, F. Hanke, P. Havu, V. Havu, X. Ren, K. Reuter, and M. Scheffler, Comp. Phys. Comm. **180**, 2175 (2009).
 - ⁵¹ S. V. Levchenko, X. Ren, J. Wieferink, R. Johanni, P. Rinke, V. Blum, and M. Scheffler, Comp. Phys. Comm. **192**, 60 (2015).
 - ⁵² A. C. Ihrig, J. Wieferink, I. Y. Zhang, M. Ropo, X. Ren, P. Rinke, M. Scheffler, and V. Blum, New J. Phys. **17**, 093020 (2015).
 - ⁵³ X. Ren, P. Rinke, V. Blum, J. Wieferink, A. Tkatchenko, A. Sanfilippo, K. Reuter, and M. Scheffler, New J. Phys. **14**, 053020 (2012).
 - ⁵⁴ F. Caruso, P. Rinke, X. Ren, A. Rubio, and M. Scheffler, Phys. Rev. B **88**, 075105 (2013).
 - ⁵⁵ T. H. Dunning, J. Chem. Phys. **90**, 1007 (1989).
 - ⁵⁶ I. Y. Zhang, P. Rinke, J. P. Perdew, and M. Scheffler, Phys. Rev. Lett. **117**, 133002 (2016).
 - ⁵⁷ D. Hirose, Y. Noguchi, and O. Sugino, Phys. Rev. B **91**, 205111 (2015).
 - ⁵⁸ J. F. Stanton, J. Gauss, N. Ishikawa, and M. Head-Gordon, J. Chem. Phys. **103**, 4160 (1995).
 - ⁵⁹ J. Oddershede, N. E. Gruner, and G. H. Diercksen, Chem. Phys. **97**, 303 (1985).
 - ⁶⁰ L. Hung, F. H. da Jornada, J. Souto-Casares, J. R. Chelikowsky, S. G. Louie, and S. Ögüt, Phys. Rev. B **94**, 085125 (2016).
 - ⁶¹ X. Ren, N. Marom, F. Caruso, M. Scheffler, and P. Rinke, Phys. Rev. B **92**, 081104 (2015).
 - ⁶² M. F. Lange and T. C. Berkelbach, J. Chem. Theory Comput. **14**, 4224 (2018).
 - ⁶³ S.-Y. Liu, K. Alnana, J. Matsumoto, K. Nishizawa, H. Kohguchi, Y.-P. Lee, and T. Suzuki, J. Phys. Chem. A **115**, 2953 (2011).
 - ⁶⁴ T. A. Carlson, P. Gerard, M. O. Krause, F. A. Grimm, and B. P. Pullen, J. Chem. Phys. **86**, 6918 (1987).